

Estimates of clear-sky solar irradiances over Nigeria

T.A. Otunla

Atmospheric Physics Research Unit, Department of Physics, University of Ibadan, Ibadan, Nigeria



ARTICLE INFO

Article history:

Received 20 February 2018

Received in revised form

16 June 2018

Accepted 11 July 2018

Available online 19 July 2018

Keywords:

Beam normal irradiance

Clear-sky diffuse irradiance

Broadband radiative model

Aerosol

Water vapour

Climate zone

ABSTRACT

This study attempts to circumvent the problem of paucity of input data required in climatology mapping of clear-sky solar irradiance in Nigeria by computing beam normal (E_{bn}) and diffuse (E_d) irradiances using a high performance broadband radiative model in the country climate zones. Air temperature, relative humidity and global datasets of ozone thickness and angstrom turbidity were used as input parameters.

The biases in the E_{bn} estimates with NASA datasets across Nigeria (11–25%) are of similar magnitudes with NASA observations with ground measurements. The estimates show persistent negative biases that increased from tropical savannah to semi-arid climate zones (–8 to –24%). The bias in the E_d estimates is only of similar magnitude with NASA in semi-arid climate zone (10%). The E_d estimates show persistent negative biases that increase from semi-arid to tropical savannah across Nigeria (–7 to –54%). Also, the estimates in each climate zone correspond to the expected climatology of water vapour, aerosol turbidity and absolute optical mass. Lastly, the response of E_{bn} to water vapour absorption and aerosol extinction signals is mostly active in monsoon zone while the response to the signals by E_d are active in all the zones.

© 2018 Elsevier Ltd. All rights reserved.

1. Introduction

Solar radiations reaching the earth's surface are usually classified as clear-sky or all sky solar irradiance. Clear-sky solar irradiance is the solar radiation that reaches the earth's surface in the absence of clouds while all sky solar irradiance includes the contribution of clouds in the radiation damping processes. In the absence of cloud, when solar radiation passes through the atmosphere, it is attenuated by five types of radiation damping processes, viz. Rayleigh scattering, aerosol extinction, ozone absorption, water vapour absorption and permanent gas absorption [1]. Efficiency of solar system is optimum and solar concentrators work only properly in clear-sky solar irradiance [2]. Other fields of studies where clear-sky solar irradiances are of primary importance include climate studies, illumination engineering, biophysical impacts of atmospheric pollution, atmospheric physics, photovoltaic and remote sensing applications [3]. Accurate predictions of the irradiance are of utmost importance to these applications. Despite this importance, there is paucity of data on clear-sky solar irradiances over extended areas in many regions of the world especially in West Africa that have virtually no stations where real time measurements are taken on continuous basis.

Modelling of the irradiance from available meteorological data is the next possible best option for locations where measurements are not available or for applications where long term time series is required. Wong and Chow [4] identified parametric and decomposition methods as the two main classes of models in literatures for predicting solar irradiances. Broadband parametric transmittance method in which the atmosphere is approximated as either one or more layers media attenuating the extra-terrestrial solar irradiance by means of several scattering and absorption processes had been used to develop a variety of models. Clear-sky solar irradiances had been modelled successfully by some of these models. For instance, Gueymard [2,5], evaluated twenty-one carefully selected parametric models against two state of the art spectral radiation transfer models and the best available beam solar irradiance data and recommend four high performance models. They are Code for Physical Computation of Radiation 2 bands (CPCR2) [6], Multilayer-Weighted Transmittance model version 2 (MLWT2) [2,5], Reference Evaluation of Solar Transmittance (REST) [2,5] and Yang model [1] (in alphabetical order). These models were found to be capable of predicting beam solar irradiance remarkably well under a variety of atmospheric conditions within the uncertainty of modern and well-maintained pyrhemometers, provided that good quality inputs of precipitable water and aerosol turbidity are used. Furthermore, in a comparative study of different beam normal solar irradiance models carried out over the Egypt

E-mail address: ta.otunla@ui.edu.ng.

atmosphere, the high performance of MLWT2, REST and Yang model were also confirmed.

Solar system applications, most especially photovoltaic are becoming proliferated in West Africa as part of renewable energy innovations because of the abundant of solar irradiance in the region due to its proximity to the equator. Designers of such systems would require accurate knowledge of distribution of solar beam irradiances across different climatic zones. Also, Clear-sky diffuse solar irradiances, which are usually a small fraction of the total (global) clear-sky solar irradiance, becomes important in high turbid environment such as semi-arid (sahel) region and during cold dry wind spell that characterised the winter climate in the West Africa. Studies on distributions of all-sky global solar irradiance over West Africa are less known to say the least. Studies dedicated to the development of the climatology for clear-sky solar irradiance over West Africa are even scarcer. It should however be pointed out that satellite data such as NASA SSE products are often been used for gap fillings [7] for the region in an attempt to develop global climatology for different atmospheric parameters. A number of studies is available in the literature on the modelling and characterisation of global solar irradiance in few locations in Nigeria. For instance, empirical models that utilised sunshine duration, temperature, and other climate elements in Angstrom-based and Hargreaves-based correlation equations, had been developed in various locations in Nigeria [8–13]. These models are site-dependent and do not explicitly account for the effect of irradiance extinction processes and optical air mass. Recently, Olayinka [14] used a regional model – International Centre for Theoretical Physics (ICTP) Regional Climate Model version 3 (RegCM3) – which utilises physically-based radiative transfer equation to simulate seasonal global solar radiation for the period 1981 to 2010 with ECHAM5 GCM as the lateral boundary conditions. A bias range of 10%–30% was obtained with NIMET and NASA observed datasets.

This study attempts to fill the gap of paucity of clear-sky solar irradiance data, using a high performance broad-band radiative transfer model by, firstly, computing clear-sky solar irradiance over Nigeria, a sub-region of West Africa and the continent's most populated sovereign state, with a clear record of energy problem; secondly, investigating the distribution of the solar irradiance over different climatic zones in the region of study; and, finally, establishing simple empirical relationships between the dominant radiative attenuation parameters and clear-sky solar irradiances that can serve climatological purposes.

2. The clear-sky model for solar irradiance estimation

The beam normal (i.e direct normal) E_{bn} [W/m^2] and clear-sky diffuse E_d [W/m^2] solar irradiances in this study were calculated from a broadband model that was first developed by Yang [1] and then further improved by Yang and Koike [15] and Yang [16]. Gueymard [2,5] evaluated 21 models and concluded that this broadband model was one of the best broadband models that is comparable to spectral radiative transfer models for calculating beam normal irradiance. Paulescu and Schlett [17] and Madkour [18] also verified the high performance of this model. The monthly daily mean of E_{bn} [W/m^2] and E_d [W/m^2] received at the ground level under clear skies, respectively are calculated as follows

$$E_{bn} = E_{on} \tilde{\tau}_b \quad (1)$$

$$E_d = E_{on} \tilde{\tau}_d \quad (2)$$

where E_{on} is the extra-terrestrial solar irradiance (i.e. the solar constant times the sun–earth distance correction factor), $\tilde{\tau}_b$ and

$\tilde{\tau}_d$ are the broadband beam and diffuse radiative transmittances, respectively. They are approximated as:

$$\tilde{\tau}_b \approx \max\left(0, \tilde{\tau}_{oz} \tilde{\tau}_g \tilde{\tau}_r \tilde{\tau}_w \tilde{\tau}_a - 0.013\right) \quad (3)$$

$$\tilde{\tau}_d \approx \max\left\{0, 0.5\left(\tilde{\tau}_{oz} \tilde{\tau}_g \tilde{\tau}_w \left(1 - \tilde{\tau}_a \tilde{\tau}_r\right) + 0.013\right)\right\} \quad (4)$$

where $\tilde{\tau}_g$, $\tilde{\tau}_r$, $\tilde{\tau}_w$, $\tilde{\tau}_a$, and $\tilde{\tau}_{oz}$ are the broadband radiative transmittances due to permanent gas absorption, rayleigh scattering, water vapour absorption, aerosol extinction and ozone absorption respectively. The detailed calculation of the transmittances can be found in the model due to Yang [1,16]. The input parameters of the model are: precipitable water (w in $g\ cm^{-2}$), angstrom turbidity, thickness of ozone layer, surface elevation (z) and air pressure (p).

3. Materials and methods of analysis

The Ångström turbidity data set was produced by the GADS (Global Aerosol Data Set 2.2a; see Refs. [19] and [20]) model. The thickness of ozone layer was obtained from TOMS (Total Ozone Mapping Spectrometer) zonal averages computed by NASA/GSFC Ozone Processing Team (see http://toms.gsfc.nasa.gov/ozone/ozone_v8.html). In the model, the precipitable water w (cm) was estimated from surface relative humidity h_r (%) and air temperature T_a (K) by a semi-empirical formula:

$$w = 0.00493 h_r T_a^{-1} \exp\left[26.23 - 5416 T_a^{-1}\right] \quad (5)$$

The air pressure was estimated from station altitude, z and surface air temperature T_a by using

$$p = p_0 \exp(-0.0342/T_a)z \quad (6)$$

Thirty years of monthly mean maximum and minimum temperature and relative humidity respectively for twenty-one meteorological stations were obtained from WMO-Regional Meteorological Research Institute, Lagos, Nigeria (widely referred to as the Nigerian Meteorological Agency (NIMET)). The meteorological stations were selected to cover and to have adequate representation of the various climate zones in Nigeria. All the locations used in the study were classified according to Köpen climate classification into warm semi-arid, monsoon and tropical savannah (Table 1). The thirty years average of the surface air temperature (T_a) and relative humidity (h_r) for every location in each climatic zone are also given in Table 1. In order to develop a simple empirical equation for the calculation of clear-sky solar irradiance, Kirchhoff's law, that is,

$$\vec{\tau}_i + \vec{\alpha}_i + \vec{\kappa}_i = 1, \quad (7a)$$

where $\vec{\tau}$, $\vec{\alpha}$ and $\vec{\kappa}$ are the transmissivity, absorptivity and reflectivity respectively, was transformed as

$$A \approx \vec{\alpha}_i = 1 - \vec{\tau}_i \quad (7b)$$

where the reflectivity due to permanent gases had been neglected and radiative scattering was assumed to be due to aerosol (a factor due to reflectivity) and it (i.e reflectivity) was also assumed to be subsumed in aerosol extinction. Equations (1) and (2) could then be written as

$$E_{ri} = 1 - \vec{\tau}_i \quad (8)$$

Table 1
The climatic zones (according to Köpen climate classification) and the stations, with the corresponding latitude, longitude, altitude, average temperature and relative humidity for the period of 30 years (1970–2000).

Climate Zone	Locations	Latitude (°N)	Longitude (°E)	Altitude(m)	Average Temperature T_a (°C)	Average Relative humidity h_r (%)
Warm Semi-arid (BSh)	Sokoto	13.02	5.25	350	29	35.7
	Gusau	12.17	6.7	463.9	27	38.4
	Katsina	12.51	7.33	492	27	32.1
	Nguru	12.93	10.48	376	27	29.3
	Maiduguri	11.85	13.08	353.8	28	32.5
	Kano	12.05	8.2	472.5	27	38.7
Monsoon (Am)	Yelwa	10.83	4.75	244	28	52.4
	Kaduna	10.6	7.45	645.4	26	47.8
	Bauchi	10.23	9.82	609.7	26	42.8
	Bida	9.1	6.02	144	29	56.2
	Minna	9.62	6.53	256.4	28	53.7
	Jos	9.87	8.9	586	22	47
	Yola	9.23	12.47	186.1	28	47.4
	Abuja	9.25	7	343.1	27	57.2
	Lagos	6.58	3.33	39.4	27	75.9
	Ibadan	7.43	3.9	227.2	27	69.1
	Oshogbo	7.78	4.48	302	26	70.2
	Benin	6.32	5.1	77.8	27	75.3
	Enugu	6.47	7.55	141.8	27	63.8
	Tropical Savanna (Aw)	Port-Harcourt	4.85	7.02	19.5	27
Calabar		4.97	8.35	61.9	27	78.1

$$E_{ri} = 1 - \frac{E_{bn}}{E_{on}} \quad (9)$$

Where i is b or d (i.e. beam normal or clear-sky diffuse solar irradiances respectively) and E_{ri} is defined as the fractional deviation of the clear-sky solar irradiance E_{bn} or E_d from E_{on} and it is related to the broadband beam normal and diffuse radiative transmittance $\bar{\tau}_b$ and $\bar{\tau}_d$ according to equation (8). Fractional deviation E_{ri} is therefore functionally related to broadband radiative attenuation A as $E_{ri} = f(A)$ or $A = f(E_{ri})$ depending on which of the two variables A and E_r is measured or approximated. The E_{ri} will therefore be used to estimate the response of the irradiances to water vapour absorption and aerosol extinction signals in the various climate zones.

3.1. Uncertainties in model estimates

There are no ground measurements of beam normal and diffuse solar irradiances in the region of the study. The performance of model estimates was therefore evaluated against satellite-based observations from NASA Surface Meteorology and Solar Energy (SSE) SSE Release (hereafter refers to as NASA SSE products). NASA SSE products are often used for gap fillings in regions where ground measurements are not available in developments of global climatology [7]. NASA SSE products were validated against ground measurement datasets whose uncertainties are not precisely known. Hence the product uncertainties are classified as mean percentage and root mean squared differences and not errors [7]. This measured of uncertainties are also utilised in this work and they are stated as follows:

Mean percentage difference (%), mpd

$$= \frac{1}{N} \sum 100(x_e - x_n)/x_n$$

Root mean squared difference (%), rmsd

$$= \sqrt{\frac{1}{N} \sum \left[100 \frac{(x_e - x_n)}{x_n} \right]^2}$$

Where x_e is the model estimate, x_n is the NASA SSE product value and N is the total number of data points.

4. Results

4.1. Beam normal and diffuse irradiance

The maximum, minimum, annual average, rainy and dry season average for E_{bn} and E_d for all the stations in each climatic zone are presented in Tables 2 and 3 respectively. Visual inspection of the tables for E_{bn} in the warm semi-arid zone indicated Maiduguri as having the highest values and Sokoto, the lowest (Table 2). For the monsoon zone, the statistics for E_{bn} were highest in Enugu and lowest in Yelwa. For tropical savannah, Table 2 indicated that the statistics of E_{bn} were higher for Port Harcourt than Calabar. The contrast was true for E_d in all the zones. The highest maximum and the highest dry season average E_d were however obtained at Katsina and Bauchi respectively as the only exception.

The monthly variations of E_{bn} and E_d for locations in warm semi-arid zone (Sokoto and Maiduguri) and a location in the north of monsoon zone (Kaduna) are given in Figs. 2a and 3a while the monthly variation of E_{bn} and E_d in tropical savannah (Port Harcourt and Calabar) and a location in the south of monsoon zone are given in Figs. 2b and 3b. Fig. 2 and Table 2 indicated that maximum values of E_{bn} which occur in the month of April for all the stations increased from Sokoto down the latitude to Port Harcourt. In the contrast, the minimum values of E_d occurred between the month of May and June, and followed a decreasing trend with latitude from Sokoto to Port-Harcourt (Table 3 and Fig. 3).

Table 2

The maximum, minimum, annual average, summer average (Rainy Season Average.) and winter average (Dry Season Average) of beam normal irradiance (E_{bn}) for all stations in each climate zone for the period of 30 years (1970–2000).

Climate zone	station	Maximum	Beam normal Irradiance, E_{bn} [W/m^2]			Dry Season Average
			Minimum.	Annual Average	Rainy Season Average	
Warm semi-arid (BSh)						
	Sokoto	278.7	194.1	244.4	261.4	230.5
	Gusau	281.0	202.2	249.9	266.7	236.2
	Katsina	286.5	200.3	249.8	263.7	237.5
	Nguru	285.2	196.1	248.9	267.7	233.9
	Maiduguri	293.9	206.3	255.8	269.1	243.7
	Kano	282.0	200.5	249.7	267.3	235.7
Monsoon (Am)						
	Yelwa	278.2	211.4	249.0	263.0	237.2
	Kaduna	279.8	212.3	251.6	266.4	238.7
	Bauchi	284.7	211.8	254.6	269.1	241.8
	Bida	285.0	219.7	258.2	271.7	246.7
	Minna	285.9	214.0	255.8	271.3	242.4
	Jos	287.5	218.7	259.5	274.1	246.8
	Yola	295.6	221.4	264.1	275.2	253.3
	Abuja	287.2	216.0	256.9	272.3	243.5
	Lagos	307.1	232.2	269.6	280.4	251.1
	Ibadan	304.4	224.7	268.4	282.3	245.7
	Oshogbo	301.0	225.8	266.2	278.7	245.7
	Benin	304.6	234.5	273.7	284.5	255.3
	Enugu	308.4	243.8	278.7	289.3	261.1
Tropical savannah (Aw)						
	Port-Harcourt	319.0	254.8	287.0	294.1	263.0
	Calabar	321.7	256.7	289.7	296.5	266.3

Table 3

The maximum, minimum, annual average, summer average (Rainy Season Average.) and winter average (Dry Season Average) of clear-sky diffuse solar irradiance (E_d) for all stations in each climate zone for the period of 30 years (1970–2000).

Climate zone	station	Maximum	Diffuse Irradiance, E_d [W/m^2]			Dry Season Average
			Minimum	Annual Average	Rainy Season Average	
Warm semi-arid (BSh)						
	Sokoto	52.2	44.4	48.8	47.1	50.0
	Gusau	51.4	40.2	47.1	44.1	49.1
	Katsina	53.2	41.6	48.2	46.5	49.5
	Nguru	52.6	43.6	48.1	46.4	49.5
	Maiduguri	50.6	40.0	44.9	43.0	46.3
	Kano	51.5	40.5	46.7	43.6	48.8
Monsoon (Am)						
	Yelwa	50.6	38.9	44.8	43.7	45.8
	Kaduna	49.6	39.5	45.3	43.3	47.0
	Bauchi	49.5	38.0	45.1	42.4	47.3
	Bida	47.6	33.7	40.5	38.8	41.8
	Minna	49.3	34.6	42.1	39.5	44.2
	Jos	49.1	37.6	44.0	40.6	46.7
	Yola	45.03	32.3	38.9	36.5	40.8
	Abuja	48.4	32.6	41.4	38.6	43.6
	Lagos	41.2	21.9	32.9	30.7	36.6
	Ibadan	42.1	25.3	34.7	32.0	39.1
	Oshogbo	44.1	27.1	35.9	34.0	38.9
	Benin	42.6	23.5	31.7	29.6	35.2
	Enugu	38.7	22.1	30.4	27.9	34.2
Tropical savanna (Aw)						
	Port-Harcourt	36.9	15.5	25.4	23.5	31.2
	Calabar	36.0	14.5	24.0	22.4	28.8

4.2. Comparison of monthly model estimates of clear-sky solar irradiance with NASA SSE observed data set

Fig. 1a and b give the monthly variations of the beam normal and diffuse solar irradiance with NASA SSE data set for all the climate zones. The model plots indicated better dynamics than the NASA SSE products. The estimates of beam normal irradiance were also indicated to be lower than NASA SSE satellite products in all the zones except for the months of March through to June in the

tropical savannah zone. The NASA SSE beam normal irradiance product was underestimated by the model with increasing values from tropical savannah to warm semi-arid (i.e. mpd increases as -8% , -13.6% -24.3% respectively). NASA SSE product also differs from the model estimates increasingly from tropical savannah to warm semi-arid with rmsd values of 11.5%, 16.9% and 25.3% respectively.

The estimates of diffuse irradiance were indicated to be lower than NASA SSE products in all the zones (Fig. 1b). The model

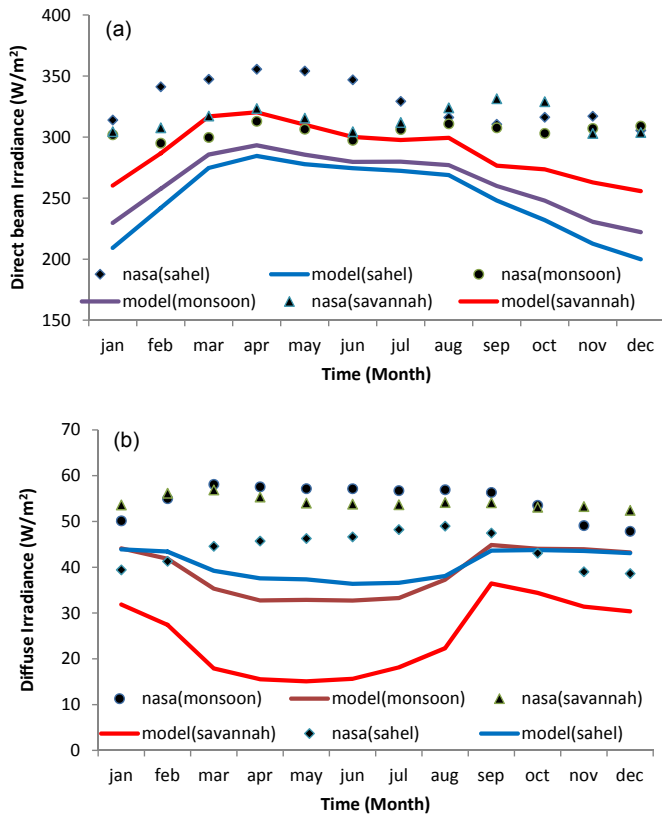


Fig. 1. a: monthly variations of beam normal irradiance from the broadband model and NASA SSE product for the periods of 1983–2005 in tropical savannah, monsoon and warm semi-arid of Nigeria. b: monthly variations of diffuse irradiance from the broadband model and NASA SSE product for the periods of 1983–2005 in tropical savannah, monsoon and warm semi-arid of Nigeria.

underestimated the NASA SSE products with decreasing mpd values of -54.3% , -27.8% and -7% for tropical savannah, monsoon and warm semi-arid zones respectively. The difference between the model and NASA SSE product also decreased from the tropical savannah to warm semi-arid with rmsd values of 56.3% , 33.2% and 16% respectively.

4.3. Aerosol and water vapour transmittances

Tables 4 and 5 give the statistics of maximum, minimum, annual average, rainy and dry season average for $\bar{\tau}_a$ and $\bar{\tau}_w$ for all the stations in each climate zones. In the warm semi-arid zone, the maximum, minimum, annual average, rainy and dry season average for $\bar{\tau}_a$ are in the range 0.22 – 0.31 , 0.14 – 0.18 , 0.19 – 0.21 , 0.20 – 0.25 and 0.18 – 0.20 respectively. In the monsoon zone, the aforementioned statistics are in the range 0.25 – 0.34 , 0.14 – 0.21 , 0.20 – 0.26 and 0.17 – 0.24 respectively. In the tropical savannah, the range of the statistics are respectively 0.47 – 0.50 , 0.18 – 0.20 , 0.33 – 0.36 , 0.34 – 0.37 and 0.29 – 0.32 .

Likewise, the range of the maximum, minimum, annual average, rainy and dry season average $\bar{\tau}_w$ in warm semi-arid zone are 0.83 – 0.84 , 0.77 – 0.78 , 0.80 – 0.81 , 0.78 – 0.79 and 0.81 – 0.83 . In the monsoon zone the statistics are in the range 0.78 – 0.82 , 0.75 – 0.78 , 0.76 – 0.80 , 0.76 – 0.78 and 0.76 – 0.82 respectively. The statistical values in the tropical savannah zone are 0.77 , 0.75 , 0.76 , 0.76 and 0.76 respectively.

The monthly variations of aerosol extinction and water vapour absorption for locations in warm semi-arid zone (Sokoto and

Maiduguri) and a location in the north of monsoon zone (Kaduna) are given in Figs. 2a and 3a while the monthly variation of aerosol extinction and water vapour absorption for locations in tropical savannah (Port Harcourt and Calabar) and a location in the south of monsoon zone are given in Figs. 2b and 3b. The highest monthly values of aerosol extinction occur in the warm semi-arid zone and decreased down the latitude to tropical savannah zone (Fig. 2 or 3). However, the highest monthly variations of aerosol extinction occur in the tropical savannah. For water vapour absorption, on the other hand, there is apparently little or no variations, especially for the months of June to October in the warm semi-arid zone and April to October in the tropical savannah zone. Higher values of water vapour absorption were, however, obtained in the lower latitude of the tropical savannah zone.

5. Discussions

The uncertainties generated for model estimate were found to be almost within the range indicated for comparison of beam normal irradiance from NASA SSE dataset with the ground measurements (i.e mpd: -12 to -3% and rmsd: 15 – 26% [7]) in all the climate zones except the semi-arid region where mpd value of -25% was obtained. For diffuse irradiance, the model estimates lied within the range obtained for the comparison of the NASA SSE product with ground measurements (i.e mpd: -5 to 5% and rmsd: 14 – 22% [7]) in the warm semi-arid zone. It should be noted that the negative mpd values reported by Chandler [7] and in this present work implied overestimation of both beam normal and diffuse irradiances by the NASA SSE dataset. Olayinka [14] also observed that NASA SSE product overestimated monthly averaged of global solar irradiance when compared with NIMET ground measurement dataset (Olayinka [14]). Thus, it could be inferred that the available ground measurement datasets indicated a tendency for NASA SSE products to overestimate solar irradiances especially in the region of study. The broadband model used in this work also indicated better dynamics than NASA SSE products as it clearly captured the irradiance monthly variations (Fig. 1a and b). The effects of solar elevation and irradiance damping processes were therefore better captured in all the climate zones.

The estimates of E_{bn} from the model decreased from tropical savannah in the south with the increase in latitude to warm semi-arid zone in the north while the converse was true for the diffuse solar irradiance. Figs. 2 and 3 indicated that both aerosol extinction and water vapour absorption changed with decreasing latitude from warm semi-arid zone in the north to tropical savannah in the south. These changes in irradiance are due to optical thickness of aerosol, water vapour and other atmospheric constituents, and the optical air mass at each location.

The effect of attenuation processes due to the presence of aerosol, water vapour and other atmospheric constituents would be discussed first. Table 4 indicated that aerosol transmittance ranged between 0.14 and 0.31 , 0.14 and 0.34 , and 0.18 and 0.50 in the warm semi-arid, monsoon and tropical savannah respectively. This would implied that 14 – 18% of E_{on} is the lowest irradiance and 31 – 50% is the highest irradiance that would reach the surface at the warm semi-arid zone and tropical savannah zone respectively if aerosol extinction were the only damping processes considered. Water vapour transmittances were also given in Table 5 to range between 0.77 and 0.84 , 0.75 and 0.83 , and 0.75 and 0.77 in the warm semi-arid, monsoon and tropical savannah respectively. By implication, if water vapour absorption was the only attenuation process considered, 75 – 77% and 77 – 84% of E_{on} were the lowest and highest irradiance that would reach the surface in the tropical savannah and warm semi-arid zones respectively. Permanent gases and ozone had little or no effect on the irradiance attenuation as

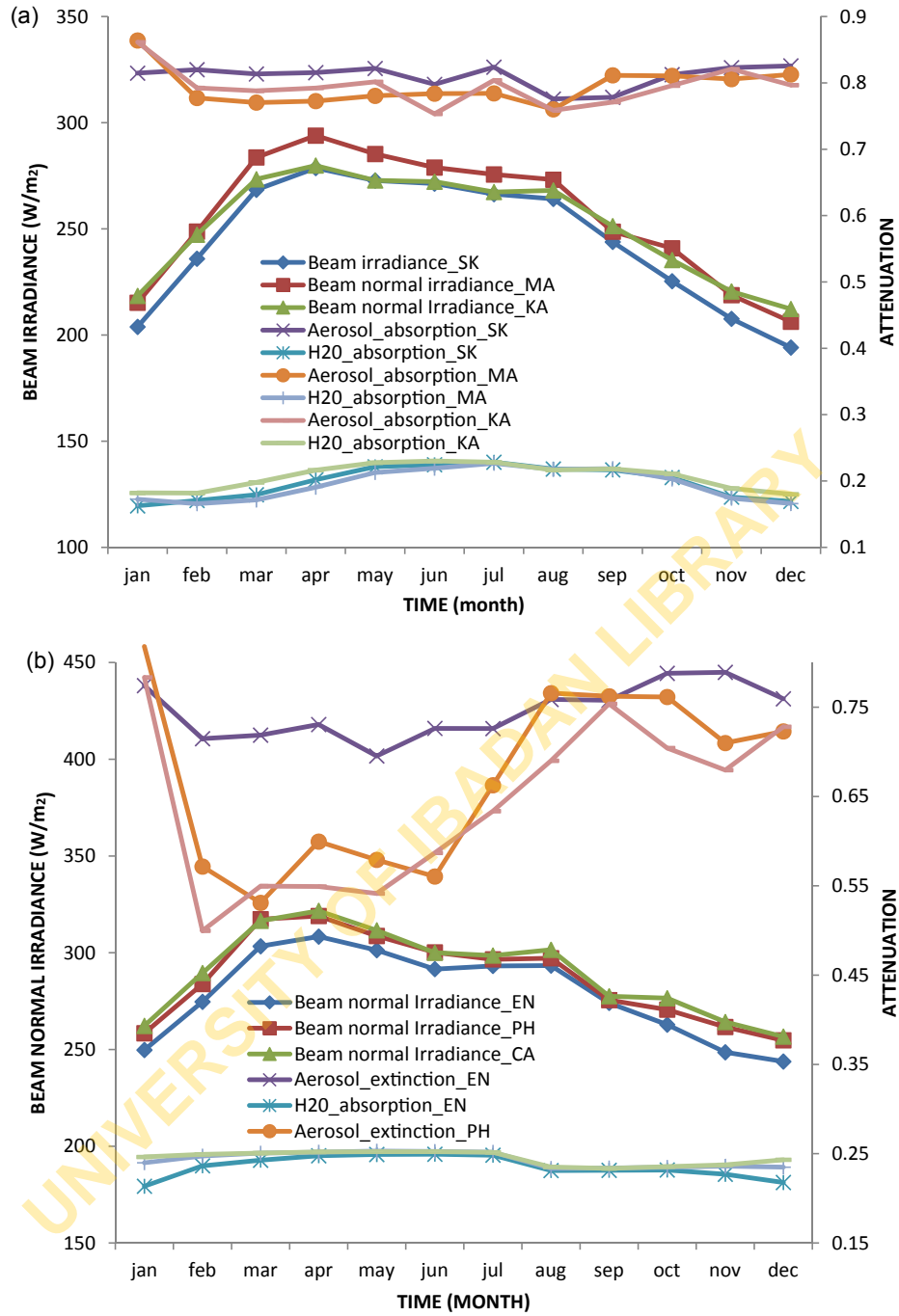


Fig. 2. a: Monthly mean variation of beam irradiance (E_{bn}) and attenuation (i.e. aerosol extinction and water vapour absorption) in Maiduguri (MA), Sokoto (SK) and Kaduna (KA) for the period of 30 years (1970–2000). b: Monthly mean variation of beam irradiance (E_{bn}) and attenuation (i.e. aerosol extinction and water vapour absorption) in Enugu (EN), Port Harcourt (PH) and Calabar (CA) for the period of 30 years (1970–2000).

their transmittances were found to be approximately closed to unity in this work. The low values of aerosol transmittance (this also implies high values of aerosol extinction if Kirchhoff's law is applied) obtained in the warm semi-arid zone was mainly due to high concentration of aerosol (harmattan dust) transported by the north-easterly wind from the Bodel Depression in the Chad Basin and other locations around the Sahara desert [21–24]. It also partly originated from the bush burning [25] in the dry season and due to agricultural practices prevalent during the transition from dry to rainy season, and from anthropogenic sources due to fossil fuel

burning. The harmattan dust were dryly deposited or rained/washed out in the southward advection into other climate zones with the implication of higher values of aerosol transmittance southward of the warm semi-arid zone. These processes of rained or washed out during the rainy season in the tropical savannah where sharp decrease in the aerosol extinction were observed (Fig. 2b or 3b), were clearly delineated from the dry deposition that mainly characterised the aerosol sink in the dry season. It should however be noted that there is always a background aerosol concentration resulting in non-zero aerosol extinction (i.e. various

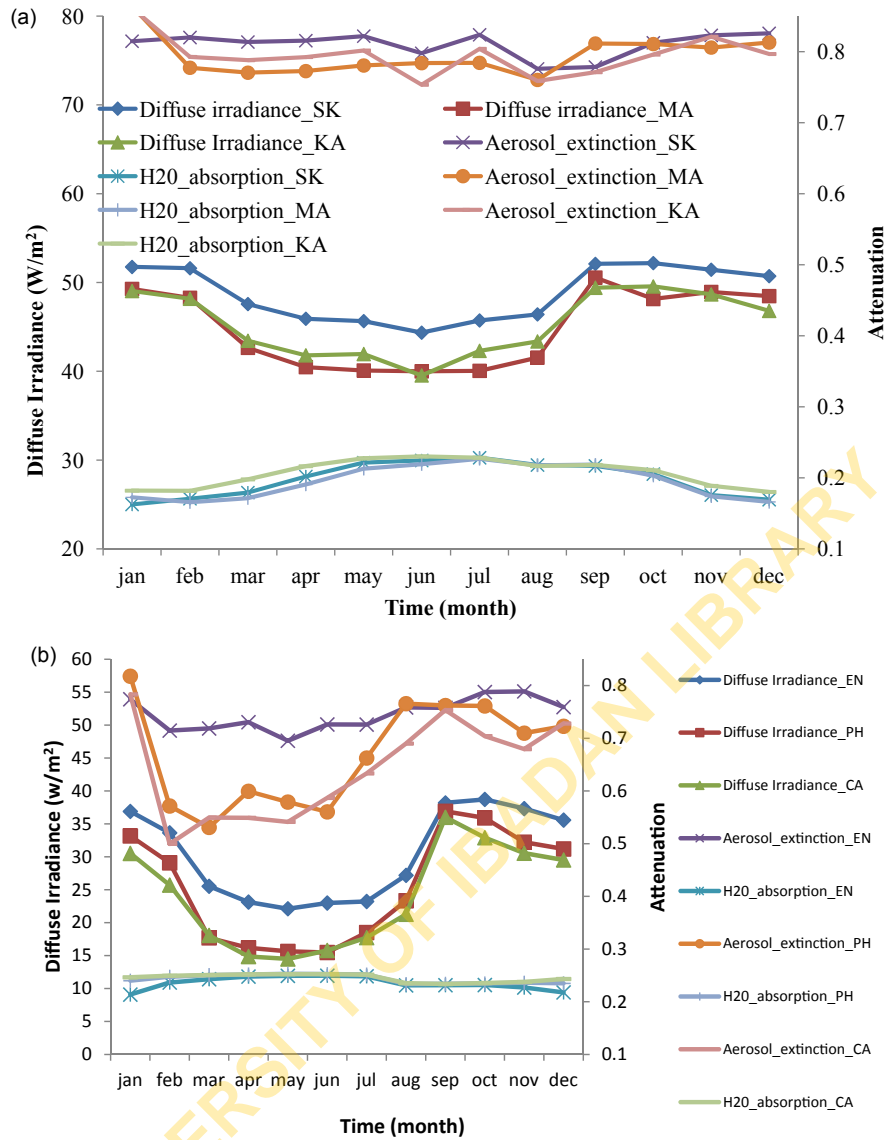


Fig. 3. a: Monthly mean variation of clear-sky diffuse solar irradiance (E_d) and attenuation (i.e. aerosol extinction and water vapour absorption) in Maiduguri (MA), Sokoto (SK) and Kaduna (KA) for the period of 30 years (1970–2000). b: Monthly mean variation of clear-sky diffuse solar irradiance (E_d) and attenuation (i.e. aerosol extinction and water vapour absorption) in Enugu (EN), Port Harcourt (PH) and Calabar (CA) for the period of 30 years (1970–2000).

statistics used in Table 4 never yielded zero aerosol transmittances) and it is highest in the warm semi-arid zone and lowest in the tropical savannah especially during the rainy season. The attenuation due to water vapour absorption was low compared to aerosol extinction, it was, notwithstanding, significant in all the climate zones as its maximum monthly transmittance values varied between 0.84 in the warm semi-arid zone and 0.77 in the moist tropical savannah zone [16]. Water vapour absorption is related to relative humidity and air temperature through Equation (5). It increased from warm semi-arid zone in the north to tropical savannah in the south.

The effects of aerosol extinction and water vapour on the attenuation of the irradiance were further illustrated in Figs. 4 and 5. Both aerosol extinction and water vapour absorption had little or no effect on the fraction deviation of E_{bn} from E_{on} (E_{rb}) in warm semi-arid zone (Fig. 4a and Table 6). For the monsoon and tropical savannah zones (Fig. 4b and c or Table 6), aerosol extinction increased linearly with E_{rb} while water vapour absorption on the

other hand indicated slight decrement. Thus, the response of E_{bn} to aerosol and water vapour forcings (signals) is mostly active in the monsoon zone.

The effects of both aerosol extinction and water vapour absorption on E_{rd} (fraction deviation of E_d from E_{on}) were significant for E_d (Fig. 5 and Table 6). The statistics of the trend line indicated that response of E_d to signals of aerosol and water vapour transmittances were active in all climate zones as indicated by the slope of the trend lines even though both the data drift (indicated by slope value greater than one) and the deviations (indicated by intercept) were greater for aerosol extinction in tropical savannah.

The absolute optical air mass m is related to altitude, z , and zenith angle, h , as [1,26]:

$$m = \frac{\exp(-0.0342z/T_a)}{[\cosh + 0.50572(96.07995 - h)^{-1.6364}]} \quad (10)$$

The absolute optical air mass for 12 noon and 7 a.m. local time

Table 4

The maximum, minimum, annual average, summer average (Rainy Season Average.) and winter average (Dry Season Average) of aerosol transmittance ($\bar{\tau}_a$) for all stations in each climate zone for the period of 30 years (1970–2000).

Climate zone	station	Maximum	Aerosol Transmittance ($\bar{\tau}_a$)			Dry Season Average
			Minimum	Annual Average	Rainy Season Average	
Warm semi-arid (BSh)						
	Sokoto	0.22	0.17	0.19	0.21	0.18
	Gusau	0.28	0.18	0.21	0.25	0.19
	Katsina	0.24	0.18	0.20	0.21	0.19
	Nguru	0.23	0.18	0.19	0.20	0.19
	Maiduguri	0.24	0.14	0.21	0.22	0.20
	Kano	0.31	0.18	0.21	0.25	0.19
Monsoon (Am)						
	Yola	0.32	0.16	0.21	0.27	0.17
	Yelwa	0.30	0.15	0.21	0.24	0.20
	Kaduna	0.25	0.14	0.21	0.22	0.19
	Bauchi	0.28	0.14	0.20	0.22	0.18
	Bida	0.31	0.15	0.22	0.22	0.21
	Minna	0.32	0.14	0.22	0.25	0.19
	Jos	0.28	0.14	0.21	0.25	0.17
	Abuja	0.34	0.15	0.21	0.24	0.19
	Lagos	0.34	0.18	0.24	0.25	0.23
	Ibadan	0.31	0.17	0.22	0.23	0.19
	Oshogbo	0.29	0.19	0.21	0.22	0.20
	Benin	0.34	0.19	0.25	0.24	0.24
	Enugu	0.30	0.21	0.26	0.26	0.24
Tropical savanna (Aw)						
	Port-Harcourt	0.47	0.18	0.33	0.34	0.29
	Calabar	0.50	0.22	0.36	0.37	0.32

Table 5

The maximum, minimum, annual average, summer average (Rainy Season Average.) and winter average (Dry Season Average) of precipitable water transmittance ($\bar{\tau}_w$) for all stations in each climate zone for the period of 30 years (1970–2000).

Climate zone	Station	Max.	Precipitable water Transmittance ($\bar{\tau}_w$)			Dry Season Ave.
			Min.	Annual Ave.	Rainy Season Ave.	
Warm semi-arid (BSh)						
	Sokoto	0.84	0.77	0.80	0.78	0.81
	Gusau	0.84	0.77	0.80	0.78	0.82
	Katsina	0.85	0.78	0.81	0.78	0.83
	Nguru	0.84	0.78	0.81	0.79	0.82
	Maiduguri	0.83	0.77	0.81	0.78	0.82
	Kano	0.83	0.77	0.80	0.78	0.81
Monsoon (Am)						
	Yola	0.81	0.77	0.78	0.77	0.79
	Yelwa	0.81	0.77	0.78	0.77	0.79
	Kaduna	0.82	0.77	0.79	0.78	0.81
	Bauchi	0.82	0.77	0.80	0.78	0.81
	Bida	0.80	0.77	0.78	0.77	0.78
	Minna	0.80	0.77	0.78	0.77	0.79
	Jos	0.83	0.78	0.80	0.78	0.82
	Abuja	0.80	0.77	0.78	0.77	0.79
	Lagos	0.78	0.75	0.76	0.76	0.76
	Ibadan	0.78	0.75	0.76	0.76	0.77
	Oshogbo	0.78	0.75	0.76	0.76	0.77
	Benin	0.77	0.75	0.76	0.76	0.76
	Enugu	0.79	0.75	0.76	0.76	0.77
Tropical savanna (Aw)						
	Port-Harcourt	0.77	0.75	0.76	0.76	0.76
	Calabar	0.77	0.75	0.76	0.76	0.75

were computed for Port Harcourt, Kaduna and Sokoto in tropical savannah, monsoon and semi-arid zones respectively and the values ranged between 0.93 and 3.

Table 7 showed that the maximum values of m (at 12 noon) obtained in January were almost constant in all the climate zones as altitude and zenith angle increased. The minimum values of m (at 12 noon) obtained in September at Port Harcourt and Kaduna were constant as altitude and zenith angle increased and only decreased by a factor of 8% from Kaduna, a station in Monsoon zone

as altitude and zenith angle further increased to Sokoto. The altitude z generally increased with the increased in latitude from the coastal stations (Table 1). However there were some marked differences as the topography of some stations along the same latitude band set them either at higher (e.g. Kaduna and Bauchi) or lower altitude (e.g. Yola). Optical air mass (at 12 noon) therefore generally remained constant in size with variations of about 0.1 from the tropical savannah in the south to warm semi-arid zone in the north with little variations for locations at lower topography. Thus, if m

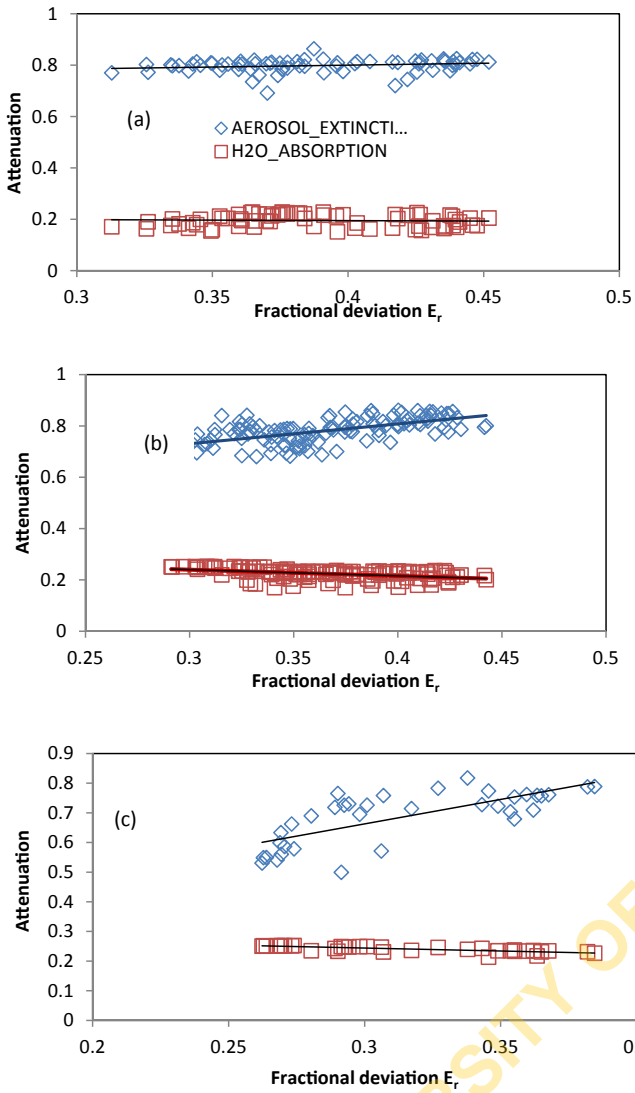


Fig. 4. Scattered plot of attenuation (i.e aerosol extinction and water vapour) against fractional deviation of monthly mean beam normal irradiance from extraterrestrial irradiance E_r of each month for (a) warm semi-arid climate zone, (b) monsoon climate zone and (c) tropical savannah zone in Nigeria.

were the only factor responsible for the radiation attenuation, there would be little variations in the values of both E_{bn} and E_d . The variations in E_{bn} and E_d in Table 7 were therefore due to the dominance of aerosol and water vapour extinction processes especially in January when aerosol concentration was highest in the region. Both E_{bn} and E_d values were almost constant across the climate zones in September (a peak point in rainy season) when the aerosol concentrations was lowest in the north. The values of E_{bn} and E_d in Kaduna, a high altitude station, indicated the contribution of both aerosol and water vapour, and the optical mass. Gueymard [5] examined the effect of different sizes of optical air mass on the attenuation of E_{bn} using both theoretical and experimental approach. He reported biases of 6.8 and 21.7% for $m = 1$ and 2, respectively (values which are very close to optical masses obtained in this work, i. e $m = 1$ and 3) for pessimistic scenario (where collocated pressure, ozone and sunphotometric or spectroradiometric data were not available and interpolations were necessary). This present study utilised similar pessimistic scenario and a high performance broadband model used in Gueymard [2,5].

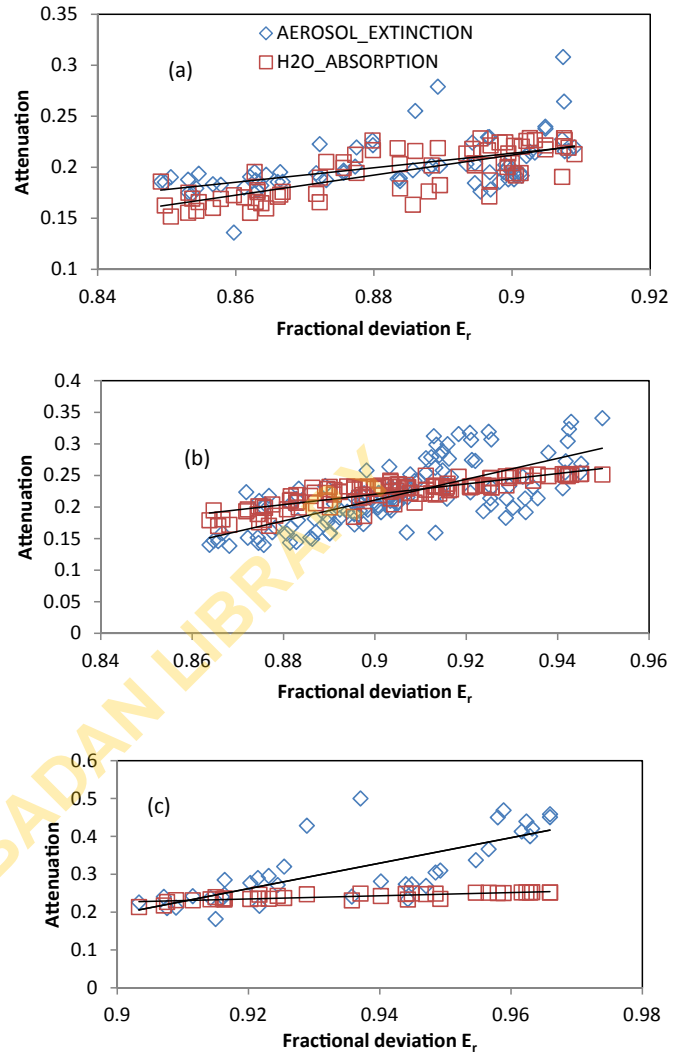


Fig. 5. Scattered plot of attenuation (i.e aerosol extinction and water vapour) against fractional deviation of monthly mean clear-sky diffuse irradiance from extraterrestrial irradiance E_r of each month for (a) warm semi-arid climate zone, (b) monsoon climate zone and (c) tropical savannah zone in Nigeria.

Table 6

Trend lines statistics of the scatter plot of attenuation (aerosol extinction and water vapour absorption) against fractional deviation of beam and diffuse irradiance from extra-terrestrial irradiance for different climates zones in the region of study.

Climate	Beam normal Irradiance [W/m ²]			Diffuse Irradiance [W/m ²]		
	Slope	intercept	R ²	slope	intercept	R ²
Aerosol extinction						
Warm semi-arid	0.15	0.74	0.04	0.71	-0.43	0.27
Monsoon	0.77	0.5	0.36	1.65	-1.27	0.49
Tropical Savannah	1.65	0.17	0.54	3.36	2.8	0.57
Water vapour absorption						
Warm semi-arid	0.04	0.21	0	0.98	-0.67	0.6
Monsoon	-0.24	0.31	0.21	0.82	-0.52	0.71
Tropical Savannah	-0.2	0.3	0.6	0.42	-0.15	0.69

6. Conclusion

A high performance parametric broadband radiative model has been used to estimate monthly averaged clear-sky solar irradiances over Nigeria, a region of West Africa. The distribution of the

Table 7

Of absolute air mass, monthly averaged diffuse irradiance and beam normal irradiance for maximum point (found in January) and minimum point (found in September) values of zenith angles in sokoto, Kaduna and Port harcourt representing the three climate zones.

station	altitude	climate zone	zenith angle		Absolute optical air		Monthly averaged Diffuse Irradiance		Monthly averaged beam normal irradiance	
			max	min	Jan.	Sept	Jan.	Sept	Jan.	Sept
Sokoto	320	semi-arid	37	10	1.0	1.2	48.3	40.7	203.9	276.6
Kaduna	645.4	Monsoon	34	8	0.9	1.1	51.3	48.0	218.4	251.3
Port harcourt	19.5	Tropical savannah	29	9	1.0	1.1	38.3	42.6	258.4	275.6

irradiance over three climate zones of tropical savannah, monsoon and warm semi-arid has been examined. The basic findings is as follows:

1. The bias in the estimates of monthly averaged beam normal irradiance for the broadband model with NASA observations across the whole country (11–25%) are of similar magnitudes with those reported for NASA observations with ground measurements. The estimates show persistent negative biases that increase from tropical savannah to warm semi-arid zones across the whole country as –8 to –24% respectively.
2. The bias in the estimates of monthly averaged diffuse irradiance for the broadband model with NASA observations is only of similar magnitudes in warm semi-arid zone (10%) with those reported for NASA observations with ground measurements. The estimates show persistent negative biases that increase from warm semi-arid to tropical savannah across the whole country as –7 to –54% respectively
3. The pattern of the estimates of clear-sky irradiances follows the expected climatology of turbidity, water vapour and optical air mass over the whole country.
4. The response of beam normal irradiance (E_{bn}) to aerosol and water vapour signals is mostly active in the monsoon zone. For diffuse irradiance, the same signals (aerosol and water vapour transmittance forcings) were however active in all the climate zones. These results could have implications for citing of baseline solar comparison network experiments in the region of study especially for beam irradiance

It is expected that the uncertainties in the model's estimates, when compared with ground-based measurements, should be lower than those obtained in comparison with NASA observations, as demonstrated in other regions of the world. Hence, there is the need to cite ground-based equipment for the direct measurements of both beam normal and clear-sky diffuse irradiance, to validate models and satellite products in West Africa.

Acknowledgements

Prof. Kun Yang of Key Laboratory of Tibetan Environment Changes and Land Surface Processes, Institute of Tibetan Plateau Research, Chinese Academy of Sciences, Beijing 100085, China provided the code for Yang model and the two auxiliary data through personal communications. Nigerian Meteorological Agency provided the routine meteorological data for the twenty-one stations used in the study.

Appendix A. Supplementary data

Supplementary data related to this article can be found at <https://doi.org/10.1016/j.renene.2018.07.053>.

References

- [1] K. Yang, G.W. Huang, N. Tamai, A hybrid model for estimating global solar radiation, *Sol. Energy* 70 (1) (2001) 13–22.
- [2] C.A. Gueymard, Direct solar transmittance and irradiance with broadband models. Part I: detailed theoretical performance assessment, *Sol. Energy* 74 (2003) 355–379.
- [3] C.P. Jacivibes, D.G. Kaskaoutis, F.S. Tymvios, D.N. Asimakopoulos, Application of SPCTRAL2 parametric model in estimating spectral solar irradiances over polluted Athena atmosphere, *Renew. Energy* 29 (2004) 1109–1138.
- [4] L.T. Wong, W.K. Chow, Solar radiation model, *Appl. Energy* 69 (3) (2001) 191–224.
- [5] C.A. Gueymard, Direct solar transmittance and irradiance predictions with broadband models. Part II: validation with high-quality measurements, *Sol. Energy* 74 (5) (2003) 381–395.
- [6] C. Gueymard, A two-band model for the calculation of clear-sky solar irradiance, illuminance and photosynthetically active radiation at the Earth's surface, *Sol. Energy* 43 (5) (1989) 253–265.
- [7] W.S. Chandler, C.H. Whitlock, P.W. Stackhouse, NASA climatological data for renewable energy assessment, *J. Sol. Energy Eng.* 126 (3) (2004) 945–949.
- [8] C.I. Ezekwe, C.C.O. Ezeilo, Measured solar radiation in a Nigerian environment compared with predicted data, *Sol. Energy* 26 (1981) 181–186.
- [9] O.A. Bamiro, Empirical relations for the determination of solar radiation in ibadan, Nigeria, *Sol. Energy* 31 (1983) 85–94.
- [10] A.A. L. Maduakwe, B. Garba, Characteristics of the monthly averaged hourly diffuse irradiance at Lagos and Zaria, Nigeria, *Renew. Energy* 17 (1999) 213–225.
- [11] L.E. Akpabio, S.E. Etuk, Relationship between global solar radiation and sunshine duration for Onne, Nigeria, *Turk. J. Phys.* 27 (2003) 161–167.
- [12] L.E. Akpabio, S.O. Udo, S.E. Etuk, Empirical correlations of global solar radiation with meteorological data for Onne, Nigeria, *Turk. J. Phys.* 28 (2004) 205–212.
- [13] M.S. Adaramola, Estimating global solar radiation using common meteorological data in Akure, Nigeria, *Renew. Energy* 47 (2012) 38–44.
- [14] O.S. Ohunakin, M.S. Adaramola, O.M. Oyewola, O.J. Matthew, R.O. Fagbenle, ScienceDirect the effect of climate change on solar radiation in Nigeria, *Sol. Energy* 116 (2015) 272–286.
- [15] K. Yang, T. Koike, A general model to estimate hourly and daily solar radiation for hydrological studies, *Water Resour. Res.* 41 (10) (2005) 1–13.
- [16] K. Yang, T. Koike, B. Ye, Improving estimation of hourly, daily, and monthly solar radiation by importing global data sets, *Agric. For. Meteorol.* 137 (1–2) (2006) 43–55.
- [17] Z. Paulescu, M. Schlett, Performance assessment of global solar irradiation models under Romanian climate, *Renew. Energy* 29 (2004) 767–777.
- [18] M.A. Madkour, M. El-Metwally, A.B. Hamed, Comparative study on different models for estimation of direct normal irradiance (DNI) over Egypt atmosphere, *Renew. Energy* 31 (3) (2006) 361–382.
- [19] P. Koepke, M. Hess, I. Schult, E. Shettle, Global Aerosol Data Set, Rep. no. 243, Max-Planck Institut für Meteorologie, 1997, p. 44.
- [20] I. Hess, M. Koepke, P. Schult, Optical properties of aerosol and clouds: the software package OPAC, *Bull. Am. Met. Soc.* 79 (1998) 831–844.
- [21] A.E. Kalu, The African dust plume: its characteristics and propagation across West – Africa in winter, in: C. Morales (Ed.), *Saharan Dust Mobilization Transport Deposit*, SCOPE, 1979, pp. 95–118.
- [22] J.M. Prospero, Long range transport of mineral dust in the global atmosphere: impact of African dust on the environment of south-Eastern United States, in: *Proceeding National Academic of Science USA*, 1999, pp. 3396–3403.
- [23] R.T. Pinker, B.N. Pandithurai, O. Holben, O. Dubovick, T.O. Aro, A dust outbreak in the sub-Sahel West Africa, *J. Geophys. Res.* 106 (2001) 922–929.
- [24] E.B. Babatunde, C.O. Akoshile, S. Garnesh, A.A. Willoughby, T.B. Ajibola, O.A. Falaiye, I.A. Adimula, T.O. Aro, Observation bio-effect of SW-global solar radiation in Ilorin in the tropics, *Adv. Space Res.* 43 (2008) 990–994.
- [25] R.T. Pinker, Y. Zhao, C.O. Akoshile, J. Janowiak, P. Arkin, Diurnal and seasonal variability of rainfall in the sub-sahel as seen from observations, satellites and numerical model, *Geophys. Res. Lett.* 33 (2006), L07806. <https://doi.org/10.1029/2005GL025192>.
- [26] F. Kasten, A.T. Young, Revised optical air mass tables and approximation formula, *Appl. Optic.* 28 (1989) 4735–4738.